PHYSICAL REVIEW E **79**, 035302(R) (2009)

Formation of regular structures in the process of phase separation

Alexei Krekhov
Physikalisches Institut, Universität Bayreuth, D-95440 Bayreuth, Germany

(Received 1 July 2008; revised manuscript received 10 February 2009; published 3 March 2009)

Phase separation under directional quenching has been studied in a Cahn-Hilliard model. In distinct contrast to the disordered patterns which develop under a homogeneous quench, periodic stripe patterns are generated behind the quench front. Their wavelength is uniquely defined by the velocity of the quench interface in a wide range. Numerical simulations match perfectly analytical results obtained in the limit of small and large velocities of the quench interface. Additional periodic modulation of the quench interface may lead to cellular patterns. The quenching protocols analyzed are expected to be an effective tool in technological applications to design nanostructured materials.

DOI: 10.1103/PhysRevE.79.035302 PACS number(s): 47.54.−r, 05.45.−a, 64.75.−g

The dynamics of phase separation in multiphase systems has been investigated intensively during the last decades [1,2]. A main paradigm are the spontaneously arising spatial concentration variations of a characteristic average domain size when a homogeneous binary mixture is quenched into the thermodynamically unstable region. With the progress of time coarsening taking place, i.e., the average domain size increases continuously. The order parameter, usually the relative concentration of the two species, obeys a conservation law in contrast to the large number of hydrodynamic pattern-forming systems [3]. For technological applications it is highly desirable to run a phase separation process in a controlled manner to create regular structures. This is important to design nanostructured materials and nanodevices in diverse fields, ranging from bioactive patterns [4] to polymer electronics [5]. The arrangement and the size of the domains which form the functional elements have a crucial impact on the device performance—e.g., in photovoltaics, light-emitting diodes (LEDs), and electronic circuits made of polymer blends [5–7]. Previous attempts to manipulate the phase separation in binary mixtures by various external fields did not lead to a satisfactory control of the pattern morphology [8–12]. A first breakthrough has been established recently by introducing a persistent spatially periodic temperature modulation in a model of the phase separation in binary mixtures [13]. In this case stripe patterns with the periodicity slaved to the externally imposed one can be stabilized against coarsening above some critical modulation amplitude.

In this paper a new effective mechanism to create periodic stripe patterns by directional quenching will be presented. Their wavelength is uniquely selected by the velocity of quench interface. If in addition a spatially periodic modulation of the quench interface is introduced, also cellular patterns can be generated.

The appropriate mean-field description of phase separation is commonly based on the generic Cahn-Hilliard (CH) model [14] (model *B* [15]). It has been widely used to study the dynamics of phase separation processes in a large variety of systems, such as binary alloys, fluid mixtures, and polymer blends [1,2]. In the one-dimensional (1D) case the CH model is described by the following partial differential equation (PDE):

$$\partial_t u = \partial_{xx}(-\epsilon u + u^3 - \partial_{xx} u), \tag{1}$$

where $u(x,t)$ is a real order parameter—e.g., in a binary mixture, the difference of concentration of one species from that at the critical point—and ϵ is the control parameter. According to Eq. (1), the spatial average $\langle u\rangle$ of $u(x,t)$ is conserved.

To keep the analysis most transparent, it is sufficient to concentrate on the case of $\langle u\rangle=0$ (the so-called critical quench). The homogeneous solution $u=0$ becomes unstable for $\epsilon>0$ against linear perturbations $\sim e^{\sigma t+iqx}$ with wave number $q\in(0,\sqrt{\epsilon})$ and growth rate $\sigma=q^2(\epsilon-q^2)$. The most unstable (fastest-growing) mode is characterized by $q_m=\sqrt{\epsilon/2}$ with $\sigma_m=\epsilon^2/4$. For $\epsilon>0$ a one-parameter family of stationary periodic solutions $u_p(x,k)$ of Eq. (1), the so-called soliton-lattice solutions, exists which can be expressed in terms of the Jacobian elliptic function sn as

$$u_p(x,k)=\frac{\sqrt{2}k}{\xi}\mathrm{sn}\left(\frac{x}{\xi},k\right),\quad \xi=\sqrt{\frac{1+k^2}{\epsilon}}. \tag{2}$$

The modulus $k\in(0,1)$ is related to the wave number q:

$$q=\frac{\pi}{2\mathrm{K}(k)\xi},\quad \mathrm{K}(k)=\int_0^{\pi/2}\frac{d\varphi}{\sqrt{1-k^2\sin^2\varphi}}, \tag{3}$$

where K is the complete Jacobian elliptic integral of the first kind. It is known, however, that any periodic solution of Eq. (1) is unstable against period doubling—i.e., against coarsening [16]. In the limit $q\ll q_m$, the growth rate of the corresponding destabilizing mode is given as [13,16]

$$\sigma_p=\epsilon^2 16\exp(-2\pi q_m/q)/(\pi q_m/q). \tag{4}$$

Note that ϵ can be scaled out in Eq. (1), which is reflected in the ϵ dependence of u_p, q, and σ_p. Coarsening becomes extremely slow, and the solutions of type (2) persist for a long time $\Delta t_p\approx 1/\sigma_p$ at small q $(k\to 1)$. This situation is favorable to the general goal of controlling phase separation to achieve long-lived periodic structures. However, with just a homogeneous quench from negative to positive values ϵ in Eq. (1), periodic structures with a single q can never be obtained: Any random perturbations about $u=0$ will develop initially into a superposition of the fastest-growing Fourier modes with average wave number $\langle q\rangle\approx q_m$. In the next stage coarsening sets in; $\langle q\rangle$ decreases continuously in time and follows a scaling law $\langle q\rangle\sim 1/\log t$ [16,17].

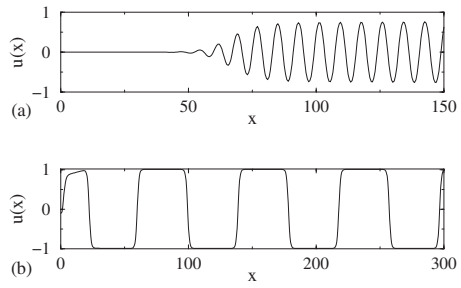

FIG. 1. Solutions of Eq. (1) with the QI (5) for $\epsilon=1$ in the comoving frame with the QI at $x=0$: $v=2>v^\star$ (a) and $v=0.02 \ll v^\star$ (b). Only a part of the system of total length $l_x=4096$ is shown.

Consequently, the question arises as to how to control the quenching process such that a quasistationary periodic solution of type (2) can be generated. It is well known that temporal and/or spatial modulations of the control parameter serve as a powerful tool to influence the pattern selection processes (see, e.g., [18,19]). One of the simplest cases is directional quenching where a jump of the control parameter is introduced and the arising interface is dragged with a constant velocity. This has motivated us to analyze systematically the impact of the directional quenching in the generic CH model. Thus we have achieved a clear understanding of controlling the generation of periodic structures. In fact, directional quenching has been used in earlier numerical simulations of certain phase separation models and some kind of regular patterns have been observed [20,21], to which we will return below. In the CH model (1), directional quenching is realized by changing ϵ from a negative value at $x<x_q$ to a positive one for $x>x_q$—i.e., dividing the system into a stable and an unstable region. The quench interface (QI) at x_q is moving in the laboratory frame with a velocity v—i.e.,

$$\epsilon(x,t)=\begin{cases}-\epsilon, & x<-vt,\\ +\epsilon, & x>-vt.\end{cases} \tag{5}$$

Numerical simulations of the 1D CH model (1) with the directional quenching (5) demonstrate that a periodic solution develops behind the QI in the unstable region. Typical examples for large and small velocities v of the QI are shown in Fig. 1: For v above some critical value $v^\star$, the periodic solution detaches from the moving QI and the wavelength of the solution becomes independent of v [Fig. 1(a)]. In contrast, for $v<v^\star$ the solution remains attached to the QI with the wavelength uniquely determined by v. Decreasing v, the solution develops into a periodic kink lattice (sharp changes between $u=\pm\sqrt{\epsilon}$) where new kinks are continuously generated at $x=x_q(t)=-vt$ [Fig. 1(b)]. The period of the solution, 2λ, turns out to be uniquely defined by velocity of the QI and is shown in Fig. 2. For $v\to 0$ one has $\lambda\sim 1/v$, whereas for $v>v^\star$ one finds $\lambda=\pi/q^\star$. Although the periodic solutions far away from the moving QI are in principle unstable against period doubling, the coarsening is extremely slow for patterns generated with $q\ll q_m$ [see Eq. (4)]. Thus the extension L_p of the (quasi-ideal) periodic solution behind the QI can be

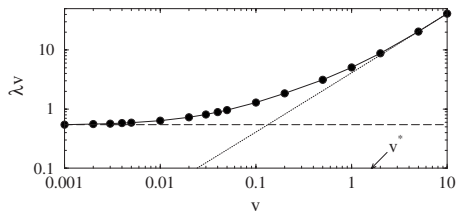

FIG. 2. Kink separation length $\lambda=\pi/q$ multiplied by the velocity v of the QI as a function of v for $\epsilon=1$ (solid circles with a solid line as a guide to the eye); $v^\star=1.622$ from Eq. (7). The dotted and dashed lines correspond to Eqs. (7) and (12), respectively.

estimated as $L_p=v\Delta t_p\approx v/\sigma_p$, where σ_p is the growth rate of the unstable period-doubling mode given in Eq. (4).

The two limiting cases of large and small velocity v of the QI can be captured analytically. For large v we consider for instance the initial condition $u=0$ everywhere except a hump $u>0$ localized near $x=0$. Then the time evolution of this initial perturbation is governed by the motion of wave fronts to the left and to the right with a well-defined velocity $v^\star$ and wave number $q^\star$. These quantities can be calculated by a linear stability analysis of the leading edge of the front in the comoving frame. One arrives thus at the so-called marginal stability criteria [18,22]

$$\frac{d\tilde{\sigma}(q_0,v^\star)}{dq}=0, \quad \mathrm{Re}[\tilde{\sigma}(q_0,v^\star)]=0, \quad q^\star=\frac{\mathrm{Im}[\tilde{\sigma}(q_0,v^\star)]}{v^\star}, \tag{6}$$

where $\tilde{\sigma}(q,v)=q^2(\epsilon-q^2)+iqv$ and q_0 is a complex number (saddle point). Equations (6) lead to the solution

$$v^\star=\frac{\sqrt{7}+2}{3}\left(\frac{2}{3}(\sqrt{7}-1)\right)^{1/2}\epsilon^{3/2},$$

$$q^\star=\frac{3(\sqrt{7}+3)^{3/2}}{8\sqrt{2}(\sqrt{7}+2)}\epsilon^{1/2}. \tag{7}$$

The phase velocity and the wave number of the propagating periodic solutions obtained from the numerical simulations of Eq. (1) for $v>v^\star$, which do not depend on v, agree perfectly with $v^\star$ and $q^\star$ given by Eq. (7) (Fig. 2).

In the opposite limit $v\to 0$, our starting point is a particular stationary solution of Eq. (1) for $v=0$ interpolating between $u=0$ at $x<0$ and $u=\sqrt{\epsilon}$ at $x>0$, which is characterized by a sharp front at $x\approx 0$. If the QI according to Eq. (5) starts to move, the sharp front would initially follow. But since the spatial average $\langle u\rangle$ is conserved regions with $u<0$ have to be generated in the region $x>x_q$, which leads to the formation of a kink lattice [Fig. 1(b)]. Its formation can be understood in terms of a fast-switching stage and a slow-pulling stage: first a new kink is generated in a short time at $x\approx x_q$. During the slow stage, this kink is pulled by the QI, whereby its amplitude and the distance to the next kink behind, $\lambda_0(t)$, increase until λ_0 exceeds some limiting value $\lambda_{0,max}$ and then a new kink is generated (Fig. 3). Repeating this process, a regular kink lattice develops in the wake of the QI with a

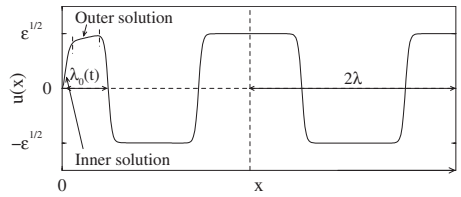

FIG. 3. Sketch of the solution of Eq. (1) with the QI (5) in the comoving frame for $x>x_q$ during the slow stage at the time shortly before the new kink will be generated at $x_q=0$. The domain of $u_{out}(x)$ connecting to u_{in} at $x=x_0$ is marked by the vertical dashes.

kink separation length λ (i.e., with the period 2λ), which is uniquely determined by the velocity v of the moving QI (Fig. 2).

During the slow stage, the solution of Eq. (1) in the interval $0\leqslant x<\lambda_0(t)$ can be described in a comoving frame $x\to x+vt$ by

$$vu = \partial_x(-\epsilon u + u^3 - \partial_{xx}u), \tag{8}$$

which is obtained from Eq. (1) by an x integration with the boundary conditions $u=0$ and zero flux $\partial_x(-\epsilon u+u^3-\partial_{xx}u)=0$ for $x=x_q=0$. In addition the explicit time dependence $\partial_t u$ can be safely neglected since it is only relevant during the fast-switching stage. The solution of Eq. (8) can be separated into a strongly varying inner solution $u_{in}(x)$ $(0\leqslant x\leqslant x_0$, first kink) and to the almost flat outer solution $u_{out}(x)$ $(x>x_0)$ (Fig. 3). For calculating u_{in} the term $vu\approx 0$ in Eq. (8) and for u_{out} the term $\partial_{xx}u\approx 0$ can be neglected, which leads to

$$(\partial_x u_{in})^2 + u_{in}^2\left(\epsilon - \frac{u_{in}^2}{2}\right) = C + 2u_{in}D,$$

$$C = (\partial_x u_{in})^2|_{x=0}, \quad D = [\partial_{xx}u_{in} + u_{in}(\epsilon - u_{in}^2)]|_{x=x_0},$$

$$\partial_x u_{out} = \frac{vu_{out}}{3u_{out}^2 - \epsilon}. \tag{9}$$

The inner and outer solutions are matched at the point $x=x_0$ chosen such that "flatness" conditions $\partial_x u_{in}=\partial_{xx}u_{in}=0$ hold. This gives for $u_0=u_{in}(x_0)$ the expression

$$u_0^2 = \frac{\epsilon}{3} + \sqrt{\left(\frac{\epsilon}{3}\right)^2 + \frac{2}{3}C}. \tag{10}$$

Starting from $u=u_0$, the outer solution u_{out} will grow until at $x=\lambda_0$ (second kink) the maximal possible amplitude $u_{max}=\sqrt{\epsilon}$ is reached. The maximal interval $\lambda_{0,max}=x_{max}-x_{min}$, where the outer solution is supported, corresponds obviously to the minimal value $u_{min}=\sqrt{2\epsilon/3}$ of u_0 [$C=0$ in Eq. (10)]. Let us now calculate the equilibrium distance between kinks λ (e.g., the distance between the third and fourth kinks in Fig. 3). During the slow-pulling stage, the distance between the second and third kinks increases until it reaches its maximal value λ when a new kink is generated at the QI. Inspection of Fig. 3 shows that then because of $\langle u\rangle=0$, the area $\lambda\sqrt{\epsilon}$ under the curve between two neighboring kinks away from the QI equals twice the area S_{max} under the curve between the first and second kinks with

$$S_{max} \equiv \int_{x_{min}}^{x_{max}} u\,dx = \int_{u_{min}}^{u_{max}} u\left(\frac{du}{dx}\right)^{-1} du. \tag{11}$$

With the use of the outer solution (9), one obtains from $\lambda\sqrt{\epsilon}=2S_{max}$

$$\lambda = 2\frac{\sqrt{6}}{9}\frac{\epsilon}{v} = 0.544\frac{\epsilon}{v}, \tag{12}$$

in perfect agreement with the results of numerical simulations in the limit $v\to 0$ (Fig. 2).

The generalization of the analysis to the off-critical quench, $\langle u\rangle\neq 0$, is straightforward. The expressions (7) for $v^\star$ and $q^\star$ hold except the replacement $\epsilon\to\epsilon-3\langle u\rangle^2$. In the limit $v\to 0$ the distances λ_+ between two kinks in the region $u>0$ and λ_- for $u<0$, respectively, become different. We find $\lambda_+-\lambda_-=\langle u\rangle\Lambda/\sqrt{\epsilon}$, and for the resulting period Λ of the kink lattice,

$$\Lambda \equiv \lambda_+ + \lambda_- = \frac{2}{v}\left[2\frac{\sqrt{6}}{9}\epsilon + \left(8 - 25\frac{\sqrt{6}}{9}\right)\langle u\rangle^2\right]. \tag{13}$$

As in the case $\langle u\rangle=0$, we found Eq. (13) confirmed in numerical simulations of Eq. (1) for different values of $\langle u\rangle$ in the limit $v\to 0$.

Let us now switch to the 2D case $u(x,y,t)$ where we study first numerically the 2D version of the CH equation (1):

$$\partial_t u = \nabla^2(-\epsilon u + u^3 - \nabla^2 u), \tag{14}$$

with the moving QI (5). Zero-flux boundary conditions have been used at $x=0,l_x$ and periodic boundary conditions at $y=0,l_y$. Initially the QI is located at $x_q=l_x$ moving from right to left. The system size was $l_x=512$, $l_y=256$, and we start with the homogeneous solution $u=\langle u\rangle$ with small superimposed noise of the strength δu where $\delta u\ll\sqrt{\epsilon}$ and $\delta u\ll\langle u\rangle$. Thus the well-known Ginzburg criterion, necessary for the validity of a mean-field description of a phase separation process [23], is satisfied: in fact, the dynamics does not depend on the particular choice of δu.

For the off-critical quench $\langle u\rangle\neq 0$, when $v<v^\star$ always regular stripe patterns with domains parallel to the QI were found [see, e.g., Fig. 4(a)]. This situation is covered by an 1D analysis presented before where the period of the structure is uniquely determined by the velocity of the QI. In the limit $v\to 0$, the period of the patterns found in our numerical simulations agree with (13). For $v>v^\star$ irregular coarsening patterns similar to the case of a spatially homogeneous quench have been observed.

In contrast, in the case of the critical quench $\langle u\rangle=0$, the orientation of the domains depends on the velocity of the QI. At small v periodic patterns with domains perpendicular to the QI are formed [similar to Fig. 4(b)]. Then, for v above $v_c\approx 0.45$, the 1D stripe patterns parallel to the QI appear as in the off-critical case described above. Finally $v>v^\star$ leads eventually to irregular patterns similar to the case of a spatially homogeneous quench.

The earlier studies of a related model subjected to directional quenching in 2D [20,21], which demonstrate the existence of regular patterns as well, were purely numerical and do not give real insight into the pattern selection mecha-

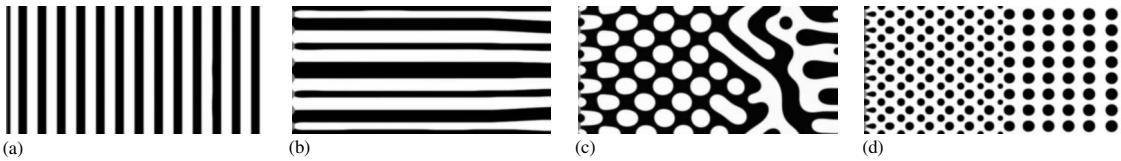

FIG. 4. Snapshots of the phase separation in 2D at the time when the QI almost reaches the left boundary. Straight QI (5) for $\epsilon=1$, $\langle u\rangle=0.1$, $v=0.05$ (a). Modulated QI (15) for $\epsilon=1$, $a=4$, $p=\pi/16$: $\langle u\rangle=0$ and $v=0.01$ (b), $v=0.055$, (c), $\langle u\rangle=0.1$, $v=0.1$ (d).

nisms. In particular, for the relevant off-critical case a noise strength $\delta u>\langle u\rangle$, violating the Ginzburg criterion, was chosen [21]. Consequently, for instance, the change of the domain orientation from perpendicular to parallel with increasing v reported in [21] is considered as an artifact.

Finally we have studied the influence of a periodic modulation of the QI which reads as follows:

$$\epsilon(x,y,t)=\begin{cases}-\epsilon, & x<l_x+a\cos(py)-vt,\\ +\epsilon, & x>l_x+a\cos(py)-vt.\end{cases} \tag{15}$$

In the case of a critical quench, we found that the velocity v_c at which the transition from parallel stripe patterns [similar to Fig. 4(a)] to perpendicular ones [Fig. 4(b)] occurs depends on the modulation amplitude a. This dependence is very strong for values a of the order of the typical domain size at the initial stage of phase separation ($a\sim\lambda_m=\pi/q_m$). Furthermore, v_c decreases with decreasing modulation wave number p. For p smaller than the wave number q_m of the fastest-growing mode, patterns with a cellular morphology forming behind the moving QI have been found [Fig. 4(c)]. In the case of an off-critical quench, we found that $\langle u\rangle\neq 0$ favors the formation of regular cellular planforms [Fig. 4(d)] at intermediate QI velocities, in analogy to the transition from parallel to perpendicular stripes for $\langle u\rangle=0$.

As a main result of the paper, we have demonstrated that directional quenching in the CH model leads to the formation of periodic solutions with the wavelength uniquely selected by the velocity of the quench interface. This is in contrast to Ginzburg-Landau models with a nonconserved order parameter where a moving quench interface leaves no kinks behind in the wake [24].

The 1D CH model has recently found a new interesting application in liquid crystals to describe Ising walls between symmetry-degenerated director configurations [25,26]. It should be possible to verify our predictions on wavelength selection by dragging the liquid-crystal layer into a homogeneous magnetic field.

In conclusion, controlling phase separation by directional quenching turns out to be a promising tool to create regular structures in material science. Although slow coarsening cannot be avoided by directional quenching in principle, long-lived periodic patterns can be "frozen in"—e.g., by a deep quench, induced polymerization, chemical treatment, etc. In this respect it would be certainly rewarding to study in more depth the 2D case where interesting cellular structures have been detected and in particular the 3D case.

I am deeply indebted to the late Lorenz Kramer from whom I have benefited a lot regarding the concept used in this paper. It is a pleasure to thank W. Pesch and W. Zimmermann for stimulating discussions and for critically reading the paper. Financial support by Deutsche Forschungsgemeinschaft Grant No. SFB 481 is gratefully acknowledged.

[1] J. D. Gunton, M. San Miguel, and P. S. Sahni, in *Phase Transitions and Critical Phenomena*, edited by C. Domb and J. L. Lebowitz (Academic, London, 1983), Vol. 8.
[2] A. J. Bray, Adv. Phys. **43**, 357 (1994).
[3] M. C. Cross and P. C. Hohenberg, Rev. Mod. Phys. **65**, 851 (1993).
[4] J. Vörös, T. Blättler, and M. Textor, MRS Bull. **30**, 202 (2005).
[5] H. Sirringhaus, Adv. Mater. (Weinheim, Ger.) **17**, 2411 (2005).
[6] D. C. Coffey and D. S. Ginger, J. Am. Chem. Soc. **127**, 4564 (2005).
[7] G. Fichet, N. Corcoran, P. K. H. Ho, A. C. Arias, J. D. MacKenzie, W. T. S. Huck, and R. H. Friend, Adv. Mater. (Weinheim, Ger.) **16**, 1908 (2004).
[8] H. Tanaka and T. Sigehuzi, Phys. Rev. Lett. **75**, 874 (1995).
[9] C. L. Emmott and A. J. Bray, Phys. Rev. E **54**, 4568 (1996).
[10] L. Berthier, Phys. Rev. E **63**, 051503 (2001).
[11] A. A. Golovin, A. A. Nepomnyashchy, S. H. Davis, and M. A. Zaks, Phys. Rev. Lett. **86**, 1550 (2001).
[12] A. Voit, A. Krekhov, W. Enge, L. Kramer, and W. Köhler, Phys. Rev. Lett. **94**, 214501 (2005).
[13] A. P. Krekhov and L. Kramer, Phys. Rev. E **70**, 061801 (2004).
[14] J. W. Cahn and J. E. Hilliard, J. Chem. Phys. **28**, 258 (1958); **31**, 688 (1959).
[15] P. C. Hohenberg and B. I. Halperin, Rev. Mod. Phys. **49**, 435 (1977).
[16] J. S. Langer, Ann. Phys. **65**, 53 (1971).
[17] T. Kawakatsu and T. Munakata, Prog. Theor. Phys. **74**, 11 (1985).
[18] W. van Saarloos, Phys. Rep. **386**, 29 (2003).
[19] S. Rüdiger, E. M. Nicola, J. Casademunt, and L. Kramer, Phys. Rep. **447**, 73 (2007).
[20] H. Furukawa, Physica A **180**, 128 (1992).
[21] B. Liu, H. Zhang, and Y. Yang, J. Chem. Phys. **113**, 719 (2000).
[22] E. Ben-Jacob, H. Brand, G. Dee, L. Kramer, and J. S. Langer, Physica D **14**, 348 (1985).
[23] K. Binder, J. Chem. Phys. **79**, 6387 (1983).
[24] N. B. Kopnin and E. V. Thuneberg, Phys. Rev. Lett. **83**, 116 (1999).
[25] C. Chevallard, M. Clerc, P. Coullet, and J.-M. Gilli, Europhys. Lett. **58**, 686 (2002).
[26] T. Nagaya and J. M. Gilli, Phys. Rev. Lett. **92**, 145504 (2004).